

Document downloaded from:

<http://hdl.handle.net/10251/102180>

This paper must be cited as:



The final publication is available at

<https://doi.org/10.1007/s11947-017-2019-8>

Copyright Springer-Verlag

Additional Information

[Click here to view linked References](#)

# NEW SPECTROPHOTOMETRIC SYSTEM TO SEGREGATE TISSUES IN MANDARIN FRUIT

Maria Victoria Traffano-Schiffo<sup>1</sup>, Marta Castro-Giraldez<sup>1\*</sup>, Ricardo J. Colom<sup>2</sup>, Pedro J. Fito<sup>1</sup>

<sup>1</sup>Instituto Universitario de Ingeniería de Alimentos para el Desarrollo, Universitat Politecnica de Valencia, Camino de Vera s/n, 46022, Valencia, Spain.

<sup>2</sup>Instituto de Instrumentación para Imagen Molecular, Universitat Politecnica de Valencia, Valencia, Spain.

**\*Corresponding author:**

Phone: +34 636998785; fax: +34 963879832.

e-mail: [marcasgi@upv.es](mailto:marcasgi@upv.es)

## Abstract

The knowledge of the electrical properties of the **fruit** tissues and their relation with the structural and compositional properties opens an endless number of opportunities in the development and design of industrial equipment for quality and **process control**. Nowadays, one of the main industrial issues is the detection of seeds inside the fruit, which could be possible with an electrical study of each tissue as a first step of the development of non-destructive sensors. In this context, a deep study of the dielectric properties of mandarin fruit tissues, coupled with  $a_w$ ,  $X_w$ , pH, maturity index, Cryo-SEM and optical measurements were performed. Dielectric properties were studied in radiofrequency and microwave ranges.  $\alpha$ ,  $\beta$  and  $\gamma$ -dispersions and **their** relaxation parameters were obtained, described and related to the chemical parameters. Finally, a **tool**, based on the relaxation dielectric constant in  $\gamma$ -dispersion able to determine the moisture content of the mandarin fruit tissues, has been developed.

**Keywords:** mandarin fruit, spectrophotometry, radiofrequency, microwave, dispersions, microstructure.

## Introduction

During the last decade, there has been a continuous increase in the consumption and demand of citrus fruits in the international market, being the mandarin fruit the one that shows the greater growth (Liu et

1  
2 al. 2012). The consumption habits promoted by a healthy diet and the nutritional qualities are some of the  
3 elements that explain this trend (Mateus-Cagua and Orduz-Rodríguez 2015).

4  
5 Histologically, mandarin fruit, as all citrus fruits, consists in three parts: peel, pulp and seed. The outer  
6 part of the peel is made up of an epidermis commonly called exocarp or flavedo and the inner part is the  
7 mesocarp or albedo. The albedo consists in vascular bundles, which are distributed along the pulp (Liu et  
8 al. 2012). The endocarp is the innermost part of the fruit and it is composed by carpels or locules (pulp)  
9 covered by slightly thick layer of vascular bundles (Goldschmidt 1988), which have a large number of  
10 juice vesicles. It is important to highlight that each tissue has different functionality, structure and  
11 composition.  
12  
13  
14  
15  
16  
17

18  
19 Regarding the composition, mandarin tissues show big differences in the content of ions, essential oils,  
20 sugars, fiber content and principally, water. It should be taken into account that each of the components  
21 aforementioned show different electric properties, which provide valuable information such as physical,  
22 chemical and compositional properties. Due to this, a spectrophotometric analysis able to describe the  
23 electric behavior of each tissue represents a first step in the development and design of industrial  
24 equipment with different applications.  
25  
26  
27  
28  
29  
30  
31

32  
33 Permittivity ( $\epsilon$ ) is the physical property which describes the interaction between the materials such as  
34 foodstuffs and a photon flux (Traffano-Schiffo et al. 2014). Expressed as a complex number, the real part  
35 of the  $\epsilon$  is called dielectric constant ( $\epsilon'$ ) and it is related to the material's ability to store energy, and the  
36 imaginary part, called dielectric loss factor ( $\epsilon''$ ) represents the energy fraction which is absorbed or  
37 dissipated (Talens et al. 2016). Along the electric spectrum between radiofrequency (RF) and microwaves  
38 (MW), three main dispersions can be observed:  $\alpha$  and  $\beta$  dispersion in radiofrequency range and  $\gamma$  in  
39 microwave range (Schwan 1957).  
40  
41  
42  
43  
44  
45  
46  
47

48  
49  $\alpha$ -dispersion (from a few Hz to a few kHz) is induced by the orientation of mobile charges in a dielectric  
50 medium (Traffano-Schiffo et al. 2017a).  $\beta$ -dispersion (from kHz to tens of MHz) is related to the  
51 orientation of fixed charges in macromolecules such as proteins and carbohydrates, and it could explain  
52 complex conformations of these molecules. At higher frequencies of  $\beta$ -dispersion the main effect is the  
53 surface tension; this phenomenon is called Maxwell-Wagner effect (Traffano-Schiffo et al. 2017a,b). In  
54 MW range, the interaction of the electric field with biological tissue produces the  $\gamma$ -dispersion. It is  
55 observed at GHz frequencies and it is due to the dipolar molecules (mainly water) orientation and  
56  
57  
58  
59  
60  
61  
62  
63  
64  
65

1 induction (Castro-Giráldez et al. 2011; Gabriel et al. 1996). Other important effect in microwave range is  
2 ionic conductivity at frequencies from Hz to MHz (Traffano-Schiffo et al. 2015). The application of a  
3 photon flux to biological tissue causes vibration of ions increasing the internal energy of the molecules,  
4 therefore, the ionic conductivity only affects to the loss factor (Castro-Giráldez et al. 2010; Castro-  
5 Giráldez et al. 2013).

6  
7  
8  
9  
10 The aim of this research is to determine the electric properties of mandarin fruit tissues in order to  
11 characterize them. This study represents a first step in the development of a method for detecting seeds  
12 inside mandarin fruit with a non-destructive method.  
13  
14  
15

## 16 17 18 **Material and methods**

### 19 20 21 **Material**

22  
23  
24 Fresh mandarins (*Citrus clementina*) obtained from a plantation located in Algimia de Alfara, Valencia,  
25 Spain were used in this experiment. Mandarins were selected according to **their** homogeneity in size and  
26 color and stored at 8 °C until **further usage**.  
27  
28  
29  
30

### 31 32 **Experimental Procedure**

33  
34 20 samples were used for the experiments. Fruits were tempered at 25 °C and the tissues (pulp, peel and  
35 **seed**) were separated and maintained in aqualab® disposable sample cups, sealed with parafilm® in order  
36 to avoid water losses. The tegument of the seeds was removed in order to avoid measurement errors due  
37 to adsorbed water to the tegument that comes from the pulp. After that, physicochemical, structural and  
38 permittivity determinations were performed. Permittivity was measured in RF range by using two sensors  
39 which consist on two **plate** electrodes (developed by the authors). In MW range a coaxial probe (Agilent)  
40 was used.  
41  
42  
43  
44  
45  
46  
47  
48  
49

### 50 51 **Physicochemical determinations**

52  
53 The pH of the pulp was measured by using a punch pH-meter S-20 SevenEasy™ (Mettler Toledo,  
54 Barcelona, Spain). A dew point Hygrometer Decagon (Aqualab®, series 3 TE) with a precision of ± 0.003  
55 was used to determine the water activity ( $a_w$ ) **at 25 °C** of each mandarin tissue. Moisture of each tissue  
56 was determined by drying in a vacuum oven at 60 °C until constant weight was reached (AOAC 2000).  
57  
58  
59  
60  
61  
62  
63  
64  
65

1 Soluble solids content of the pulp liquid phase was determined by measuring the refractometric index  
2 (°Brix) with a refractometer (ABBE, ATAGO Model 3-T, Japan) calibrated with distilled water at 25 °C.

3  
4 Titratable acidity, expressed as citric acid in 100 mL of juice, was analyzed following AOAC Method  
5 934.06 titrating an aliquot of juice with 0.1 N NaOH (AOAC 2000).  
6

7 Analytical determinations described above were obtained in triplicate.  
8

9 Finally, maturity index (MI) was calculated by dividing the soluble solids content of the extractable juice  
10 by its titratable acidity (Melgarejo et al. 2017; Alférez et al. 2005).  
11  
12

### 13 14 **Structural analysis**

15  
16 Low-temperature scanning electron microscopy (Cryo-SEM).  
17

18  
19 The microstructure of each fruit tissue was analyzed by Cryo-SEM. A Cryostage CT-1500C unit (Oxford  
20 Instruments, Witney, UK), coupled to a Jeol JSM-5410 scanning electron microscope (Jeol, Tokyo,  
21 Japan), was used. The sample was immersed in slush N<sub>2</sub> (-210 °C) and then quickly transferred to the  
22 Cryostage at 1 kPa where sample fracture took place. The sublimation (etching) was carried out at -95 °C.  
23 The final point was determined by direct observation in the microscope, working at 5 kV. Then, once  
24 again in the Cryostage unit, the sample was coated with gold in vacuum (0.2 kPa), applied for 3 min, with  
25 an ionization current of 2 mA. The observation in the scanning electron microscope was carried out at 20  
26 kV, at a working distance of 15 mm and a temperature ≤ -130 °C.  
27  
28  
29  
30  
31  
32  
33  
34  
35  
36

### 37 38 **Optical measurements**

39  
40 Optical measurements of each fruit tissue were made by a binocular loupe Leica MZ APO™ (Leica  
41 Microsystems, Wetzlar, Germany) with low magnification (8x to 80x) using incident light illumination  
42 (light reflected off the surface of the sample). It uses two separate optical paths with two objectives and  
43 two eyepieces to provide slightly different viewing angles to the left and right eyes. In this way, it allows  
44 a three-dimensional visualization of the sample.  
45  
46  
47  
48  
49  
50

### 51 52 **Permittivity Measurements**

#### 53 54 **Radiofrequency range**

55  
56 Two different non-destructive sensors developed by The Institute of Food Engineering for Development  
57 (IuIAD) and The Institute for Molecular Imaging Technologies (I3M), both at the Polytechnic University  
58  
59  
60  
61  
62  
63  
64  
65

1 of Valencia (Spain) were used to measure the permittivity in radiofrequency range. Sensors consist of two  
2 flat plates electrodes with different dimensions of the plates (Figure 1a), which were connected to an  
3 impedance analyzer Agilent 4294A (Agilent, Santa Clara, CA, USA). The measured frequency range was  
4 from 40 Hz to 1 MHz. Calibration of the equipment was performed in open (air) and short-circuit.  
5  
6 The signal obtained by the Agilent analyzer is the impedance  $Z$ , which was transformed to permittivity as  
7  
8 was described by Traffano-Schiffo et al. (2017a).  
9  
10  
11  
12  
13

#### 14 Microwave range

15  
16 Permittivity in microwave range was measured from 500 MHz to 20 GHz with an Agilent 85070E open-  
17 ended coaxial probe (Agilent, Santa Clara, CA, USA) (Figure 1b) connected to an Agilent E8362B  
18 Vector Network Analyzer (Agilent, Santa Clara, CA, USA). The system was calibrated using three  
19 different types of loads: open (air), short-circuit and 25 °C Milli<sup>®</sup>-Q water. Once the calibration was  
20 carried out, 25 °C Milli<sup>®</sup>-Q water was measured again to check calibration suitability.  
21  
22  
23  
24  
25  
26

27 Permittivity measurements were performed in triplicate.  
28  
29  
30

31 **Fig. 1** Schematic representation of the sensors used at different frequency ranges. a. radiofrequency and b.  
32 microwave  
33  
34  
35  
36  
37  
38

#### 39 Statistical analysis

40  
41 The statistical analysis was carried out with the Statgraphics Centurion XVI Software (Statgraphics,  
42 Warrenton, VA, USA). One-Way ANOVA analyses were made in order to find statistically significant  
43 differences between the parameters studied for the different samples. The logistic model developed by  
44 Traffano-Schiffo and co-workers was used in order to fit the dielectric constant spectra by using nonlinear  
45 regression (Traffano-Schiffo et al. (2017a).  
46  
47  
48  
49  
50  
51  
52

#### 53 Results and discussion

54  
55 The macro and microstructural analysis of mandarin fruit can be observed in Figure 2, where big  
56 differences among the different types of tissues can be appreciated. Firstly, the peel is composed by the  
57 flavedo, which is the outer part of the peel, and the albedo, the inner part. The flavedo is constituted by  
58  
59  
60  
61  
62  
63  
64  
65

1 the epidermis which is covered by a cuticle, while inward parenchymatic cells can be appreciated. The  
2 parenchymatic cells are isodiametric and have spherical or oval shapes with very compacted structure,  
3 where practically does not exist intercellular spaces and thus the liquid phase inside is very low. These  
4 cells are found below the epidermis and surrounding oil glands cavities (trichomes). Furthermore, the  
5 importance of flavedo is that it contains the stomas, which are cellular complex responsible for the gas  
6 exchange between the interior and exterior of the fruit. Therefore, the flavedo shows various functions,  
7 first the outer part or cuticle reduces the water exchange with the outside, maintaining high internal water  
8 activity, and on the other hand, the stomas (indicated by an arrow) are surrounded by two cells defined as  
9 guard or occlusive cells, which regulate the opening of the stoma by integrating different signals  
10 (endogenous or exogenous). Proper stoma regulation provides an efficient use of water and optimum CO<sub>2</sub>  
11 exchange rate (Ladanyia, 2008).

12  
13  
14  
15  
16  
17  
18  
19  
20  
21  
22  
23 The albedo is the inner and white part of the peel and it consists in meristematic cells, with irregular  
24 shape and size and with large air gaps. The cells have tubular geometry, which are interconnected with  
25 large intercellular spaces. Macroscopically, tubular geometry can be correlated with a spongy structure,  
26 free of turgidity and compartmentalization. With regard to the pulp, it is composed by lengthened cells  
27 called vesicles, where most of its space is occupied by vacuoles, which contain the majority of the liquid  
28 phase of the system (juice reservoir) and where the sugars and the organic acids, such as citric acid  
29 produced during the ripening, are stored. Finally, seed cells show a very tightly packed structure with  
30 very low liquid phase.

31  
32  
33  
34  
35  
36  
37  
38  
39  
40  
41  
42  
43 **Fig. 2** Overview of the macro and microstructure of mandarin

44  
45  
46  
47  
48  
49 It should be taken into account that the physicochemical parameters greatly affect the electrical  
50 properties, so, in Table 1 these parameters, segregated according to the MI of the fruits, can be observed.  
51 Both the moisture and the water activity show significant differences ( $p < 0.05$ ) between the tissues.

52  
53  
54  
55  
56 The dielectric properties of a biological tissue result from the interaction between its constituents at  
57 cellular and molecular level and the photon flux (Kuang and Nelson 1998). Permittivity was measured in  
58 RF and MW ranges, however, one of the main problems to fit the full spectrum is the appearance of three  
59

1 dispersions ( $\alpha$ ,  $\beta$  and  $\gamma$ ) on a very large frequency range with sigmoidal shape. Traffano-Schiffo et al.  
2 (2017a) developed a modified Gompertz model to describe the dielectric constant spectra. This model  
3 allows determining the dielectric constants and the relaxation frequencies of each dispersion (Tables 2  
4 and 3, respectively). Relaxation parameters are important because they allow characterizing the dielectric  
5 behavior of biological tissues (Traffano-Schiffo et al. 2017b). Figure 3 shows the average data obtained  
6 for the three characteristic dispersions of the different types of mandarin tissues.  
7  
8  
9  
10  
11  
12  
13  
14  
15

16 **Fig. 3** Dielectric constant spectra of the different mandarin tissues. Where: the lines correspond to the  
17 values of the mathematical model and the points to the average of the experimental data. (---) corresponds  
18 to the pulp, (—) the peel and (—) the seed  
19  
20  
21  
22  
23  
24  
25

26 As Figure 3 and Table 2 show, the dielectric constant of the pulp is higher than those of the peel and the  
27 seed along the spectrum. Particularly, in  $\alpha$ -dispersion the dielectric constant of relaxation of the pulp  
28 shows a significant higher value ( $p < 0.05$ ) than the other tissues due to the fact that the pulp is rich in  
29 electrolytes such as  $\text{Ca}^{2+}$ ,  $\text{Mg}^{2+}$ ,  $\text{K}^+$ ,  $\text{Na}^+$ ,  $\text{Fe}^{3+}$ ,  $\text{Cu}^{2+}$ ,  $\text{Mn}^{2+}$  and  $\text{Zn}^{2+}$  (Pérez-López et al. 2007) (with high  
30 mobility) and highly electronegative organic acids (citric and ascorbic acids) (Traffano-Schiffo et al.  
31 2016; 2017c; 2017d); all solved in liquid phase, which increase the dielectric constant of relaxation. In  
32 contrast, in both peel and seed, the ion content with mobility is low, thus the signal decreases  
33 considerably and no significant differences between both samples can be appreciated (Table 2). However,  
34 the relaxation frequency in this spectrum range (Table 3) shows significant differences among all the  
35 tissues ( $p < 0.05$ ), which means that the use of the relaxation frequency in  $\alpha$ -dispersion could represent a  
36 useful tool for tissue differentiation.  
37  
38  
39  
40  
41  
42  
43  
44  
45  
46  
47

48 With regard to  $\beta$ -dispersion, there are no significant differences ( $p < 0.05$ ) between seed and peel in terms  
49 of the dielectric constant of relaxation (Table 2).  $\beta$ -dispersion can be understood by the orientation of the  
50 fixed charges of proteins or carbohydrates which have active sites and orientation capacity (Traffano-  
51 Schiffo et al. 2017a). The seeds are composed by proteins (in low proportions) and the peel presents high  
52 carbohydrates content, however it seems that they do not present orientation capacity, thus the signal in  
53  
54  
55  
56  
57  
58  
59  
60  
61  
62  
63  
64  
65



1 both cases is low. In addition, the only samples that show significant differences ( $p < 0.05$ ) in  $\beta$ -relaxation  
2 frequency are peel and pulp (Table 3).  
3

4  
5 Finally, in the spectrum range of the  $\gamma$ -dispersion, significant differences ( $p < 0.05$ ) in the dielectric  
6 relaxation constant between the three types of tissues can be observed (Table 2). As was explained in the  
7 introduction,  $\gamma$ -dispersion is related with the orientation and induction of dipolar molecules (water) and as  
8  
9 Table 1 shows there are significant differences in moisture and water activity for all samples ( $p < 0.05$ ),  
10  
11 being the pulp **the one** which presents the highest values and the seed, the lowest. In addition, also the  
12  
13 micrographies (Figure 2) show differences in water content among tissues. Thus, microwave range can be  
14  
15 considered as the optimum range to differentiate mandarin tissues and therefore, a deep analysis is  
16  
17 needed.  
18  
19  
20  
21

22 Taking into account the imaginary part of the permittivity, the dielectric loss factors of the different  
23 mandarin tissues are shown in Figure 4. At low frequencies of the microwave range, the effect of the  
24 ionic conductivity can be appreciated. Ionic conductivity produces vibration of charged molecules;  
25 therefore, it only produces electrical energy losses (Talens et al. 2016; Castro-Giráldez et al. 2010). It  
26 should be noted that the pulp presents the highest ionic effect due to the high ions concentration (Pérez-  
27 López et al. 2007) which generate vibrations when the tissue is subjected to an external electric field  
28 (Traffano-Schiffo et al. 2015).  
29  
30  
31  
32  
33  
34  
35  
36  
37  
38  
39

40 **Fig. 4 Dielectric loss factor in MW ranges. Where: (▲) corresponds to the pulp, (●) the peel and (◆) the**  
41 **seed**  
42  
43  
44  
45  
46  
47

48 Figure 5 shows the relations between the logarithm of the moisture in dry basis and the dielectric constant  
49 in  $\gamma$ -relaxation, where it is possible to observe a linear relation between both parameters ( $R^2 = 0.948$ ).  
50 Therefore, the relaxation dielectric constant in  $\gamma$ -dispersion is a useful tool to predict the moisture in dry  
51 basis by using dielectric spectroscopy.  
52  
53  
54  
55  
56  
57  
58  
59  
60  
61  
62  
63  
64  
65

1  
2 **Fig. 5** Evolution of the relaxation dielectric constant in  $\gamma$ -dispersion with regard to the moisture for the  
3 different tissues. Where: ( $\blacktriangle$ ) corresponds to the pulp, ( $\bullet$ ) the peel and ( $\blacklozenge$ ) the seed  
4  
5  
6

## 7 **Conclusions**

8  
9  
10 It is possible to study deeply all mandarin tissues at macroscopic and microscopic level, to understand and  
11 to relate the structure with physicochemical and electric properties. The relaxations parameters (dielectric  
12 constant and frequency) of each tissue in  $\alpha$ ,  $\beta$  and  $\gamma$ -dispersions are obtained. Finally, a tool based on the  
13 relaxation dielectric constant in  $\gamma$ -dispersion, able to determine the moisture of the samples in dry basis, is  
14 developed.  
15  
16  
17  
18  
19

20  
21 This investigation work represents a valuable first step in the design and development of non-invasive and  
22 on-line sensors for detecting seeds inside the mandarin fruit based on a spectrophotometric analysis at  
23 microwave range.  
24  
25  
26  
27

## 28 **Acknowledgements**

29  
30 The authors acknowledge the financial support from: the Spanish Ministerio de Economía, Industria y  
31 Competitividad, Programa Estatal de I+D+i orientada a los Retos de la Sociedad AGL2016-80643-R,  
32 Agencia Estatal de Investigación (AEI) and Fondo Europeo de Desarrollo Regional (FEDER). Maria  
33 Victoria Traffano Schiffo wants to thank the FPI Predoctoral Program of the Universidad Politécnica de  
34 Valencia for its support. The authors would like to thank the Electronic Microscopy Service of the  
35 Universidad Politécnica de Valencia for its assistance in the use of Cryo-SEM and also Multiscan  
36 Technologies S.L. for their support.  
37  
38  
39  
40  
41  
42  
43  
44  
45  
46  
47

## 48 **References**

49  
50  
51 Alférez, F., Sala, J.M., Sanchez-Ballesta, M.T., Mulas, M., Lafuente, M.T., Zacarias, L. (2005). A  
52 comparative study of the postharvest performance of an ABA-deficient mutant of oranges: I.  
53 Physiological and quality aspects. *Postharvest Biology and Technology*, 37(3), 222-231.  
54  
55  
56  
57  
58 AOAC, (2000). AOAC, Association of Official Analytical Chemist Official Methods of Analysis.  
59 Washington, D.C.  
60  
61  
62  
63  
64  
65

1 Castro-Giráldez, M., Fito, P.J., Chenoll, C., Fito, P. (2010). Development of a dielectric spectroscopy  
2 technique for determining key chemical components of apple maturity. *Journal of Agricultural and Food*  
3 *Chemistry*, 58(6), 3761-3766.  
4

5  
6 Castro-Giráldez, M., Fito, P.J., Fito, P. (2010). Application of microwaves dielectric spectroscopy for  
7 controlling pork meat (*Longissimus dorsi*) salting process. *Journal of Food Engineering*, 97(4), 484-490.  
8  
9

10  
11 Castro-Giráldez, M., Fito, P.J., Fito, P. (2011). Application of microwaves dielectric spectroscopy for  
12 controlling long time osmotic dehydration of parenchymatic apple tissue. *Journal of Food Engineering*,  
13 104(2), 227-233.  
14  
15  
16

17  
18 Castro-Giráldez, M., Fito, P.J., Ortolá, M.D., Balaguer, N. (2013). Study of pomegranate ripening by  
19 dielectric spectroscopy. *Postharvest Biology and Technology*, 86, 346-353.  
20  
21  
22

23 Gabriel, S., Lau, R.W., Gabriel, C. (1996). The dielectric properties of biological tissues: III. Parametric  
24 models for the dielectric spectrum of tissues. *Physics in Medicine and Biology*, 41(11), 2271.  
25  
26  
27

28 Goldschmidt, E.E. (1988). Regulatory aspects of chloro-chromoplast interconversions in senescing Citrus  
29 fruit peel. *Israel Journal of Botany*, 37(2-4), 123-130.  
30  
31  
32

33 Kuang, W., Nelson, S.O. (1998). Low-frequency dielectric properties of biological tissues: a review with  
34 some new insights. *Transactions of the ASAE-American Society of Agricultural Engineers*, 41(1), 173-  
35 184.  
36  
37  
38  
39

40 **Ladanya, M. S. (2008). Citrus fruit: biology, technology and evaluation. USA: Academic Press.**

41  
42  
43 Liu, Y., Heying, E., Tanumihardjo, S.A. (2012). History, global distribution, and nutritional importance  
44 of citrus fruits. *Comprehensive Reviews in Food Science and Food Safety*, 11(6),530-545.  
45  
46  
47

48 Mateus-Cagua, D., Orduz-Rodríguez, J.O. (2015). Mandarina Dancy: una nueva alternativa para la  
49 citricultura del piedemonte llanero de Colombia. *Corpoica Ciencia y Tecnología Agropecuaria*, 16, 105-  
50 112.  
51  
52  
53  
54

55 **Melgarejo, P., Legua, P., Pérez-Sarmiento, F., Martínez-Font, R., Martínez-Nicolás, J.J., Hernández, F.**  
56 **(2017). Effect of a New Remediated Substrate on Fruit Quality and Bioactive Compounds in Two**  
57 **Strawberry Cultivars. *Journal of Food and Nutrition Research*, 5, 579-586.**  
58  
59  
60  
61  
62  
63  
64  
65

1 Pérez-López, A.J., López-Nicolás, J.M., Carbonell-Barrachina, A.A. (2007). Effects of organic farming  
2 on minerals contents and aroma composition of Clemenules mandarin juice. *European Food Research*  
3 *and Technology*, 225(2), 255-260.  
4

5  
6 Schwan, H.P. (1957). Electrical properties of tissue and cell suspensions. *Advances in Biological and*  
7 *Medical Physics*, 5, 147.  
8  
9

10  
11 Talens, C., Castro-Giraldez, M., Fito, P.J. (2016). Study of the effect of microwave power coupled with  
12 hot air drying on orange peel by dielectric spectroscopy. *LWT-Food Science and Technology*, 66, 622-  
13 628.  
14  
15  
16

17  
18 Traffano-Schiffo, M.V., Balaguer, N., Castro-Giráldez, M., & Fito, P.J. (2014). Emerging Technologies  
19 in Fruit Juice Processing. In A. Ibartz, V. Falguera (Eds), *Juice processing: Quality, safety and value-*  
20 *added opportunities* (pp. 197-212). Boca Raton: CRC Press.  
21  
22  
23

24  
25 Traffano-Schiffo, M.V., Castro-Giraldez, M., Colom, R.J., Fito, P.J. (2017a). Development of a  
26 Spectrophotometric System to Detect White Striping Physiopathy in Whole Chicken Carcasses. *Sensors*,  
27 17(5), 1024.  
28  
29  
30

31  
32 Traffano-Schiffo, M.V., Castro-Giraldez, M., Colom, R.J., Fito, P.J. (2017b). Innovative  
33 spectrophotometric system to determine chicken meat quality. *Innovative Food Science and Emerging*  
34 *Technologies*.  
35  
36  
37

38  
39 Traffano-Schiffo, M.V., Castro-Giraldez, M., Colom, R.J., Fito, P.J. (2015). Study of the application of  
40 dielectric spectroscopy to predict the water activity of meat during drying process. *Journal of Food*  
41 *Engineering*, 166, 285-290.  
42  
43  
44

45  
46 Traffano-Schiffo, M.V., Laghi, L., Castro-Giraldez, M., Tylewicz, U., Rocculi, P., Ragni, L., Dalla Rosa,  
47 M., Fito, P.J. (2017c). Osmotic dehydration of organic kiwifruit pre-treated by pulsed electric fields and  
48 monitored by NMR. *Food Chemistry*, 236, 87-93. <https://doi.org/10.1016/j.foodchem.2017.02.046>  
49  
50  
51

52  
53 Traffano-Schiffo, M.V., Laghi, L., Castro-Giraldez, M., Tylewicz, U., Romani, S., Ragni, L., Dalla Rosa,  
54 M., Fito, P.J. (2017d). Osmotic dehydration of organic kiwifruit pre-treated by pulsed electric fields:  
55 Internal transport and transformations analyzed by NMR. *Innovative Food Science and Emerging*  
56 *Technologies*, 41, 259-266.  
57  
58  
59  
60  
61  
62  
63  
64  
65

Traffano-Schiffo, M.V., Tylewicz, U., Castro-Giraldez, M., Fito, P.J., Ragni, L., Dalla Rosa, M. (2016).  
Effect of pulsed electric fields pre-treatment on mass transport during the osmotic dehydration of organic  
kiwifruit. *Innovative Food Science and Emerging Technologies*, 38, 243-251.

1  
2  
3  
4  
5  
6  
7  
8  
9  
10  
11  
12  
13  
14  
15  
16  
17  
18  
19  
20  
21  
22  
23  
24  
25  
26  
27  
28  
29  
30  
31  
32  
33  
34  
35  
36  
37  
38  
39  
40  
41  
42  
43  
44  
45  
46  
47  
48  
49  
50  
51  
52  
53  
54  
55  
56  
57  
58  
59  
60  
61  
62  
63  
64  
65

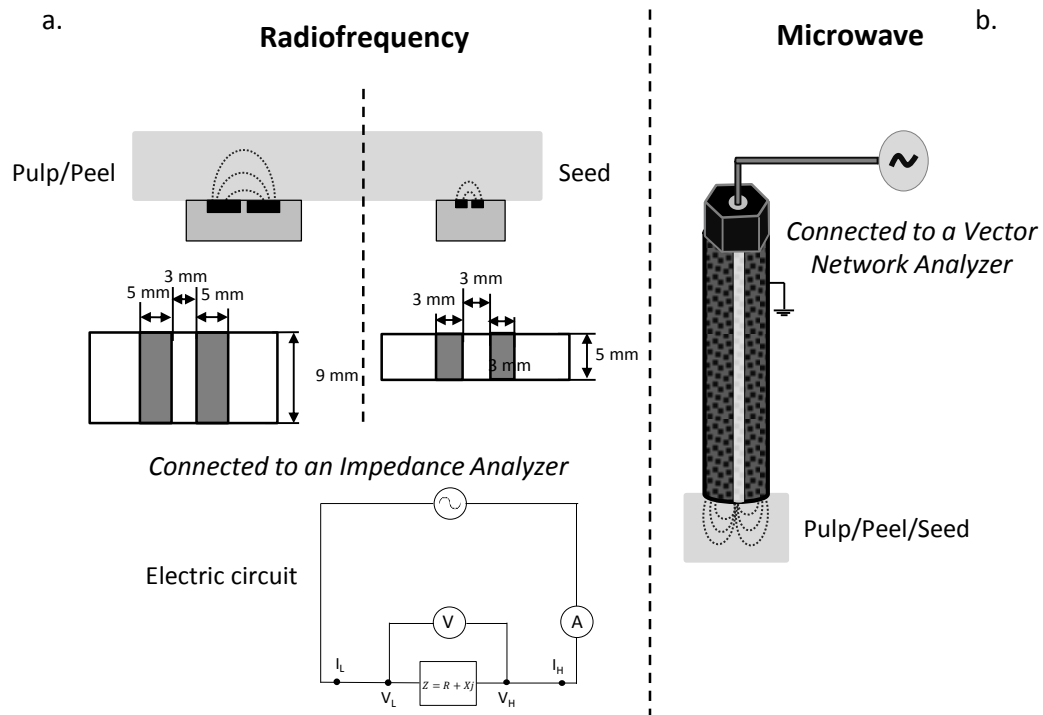


**Fig. 1**

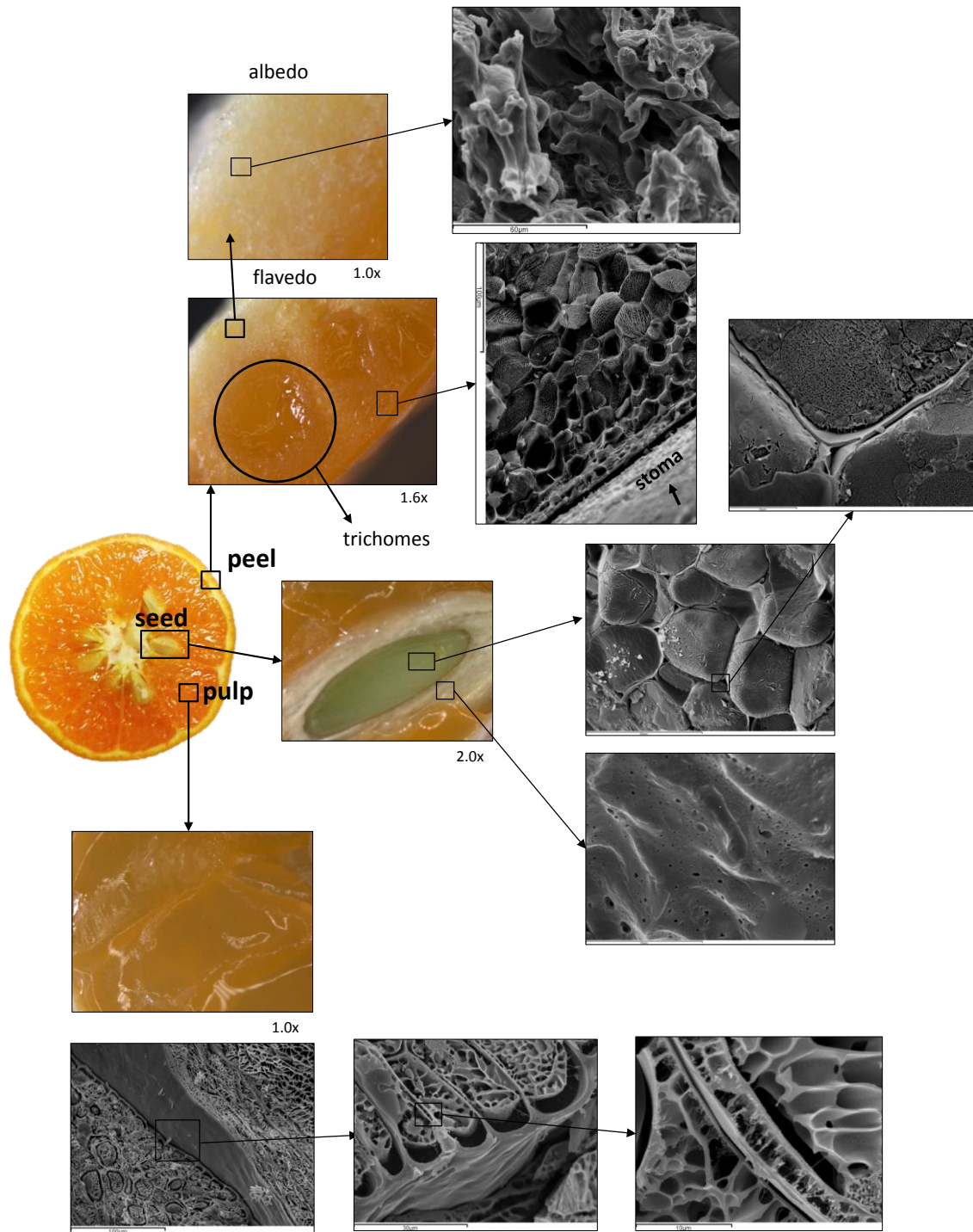


**Fig. 2**

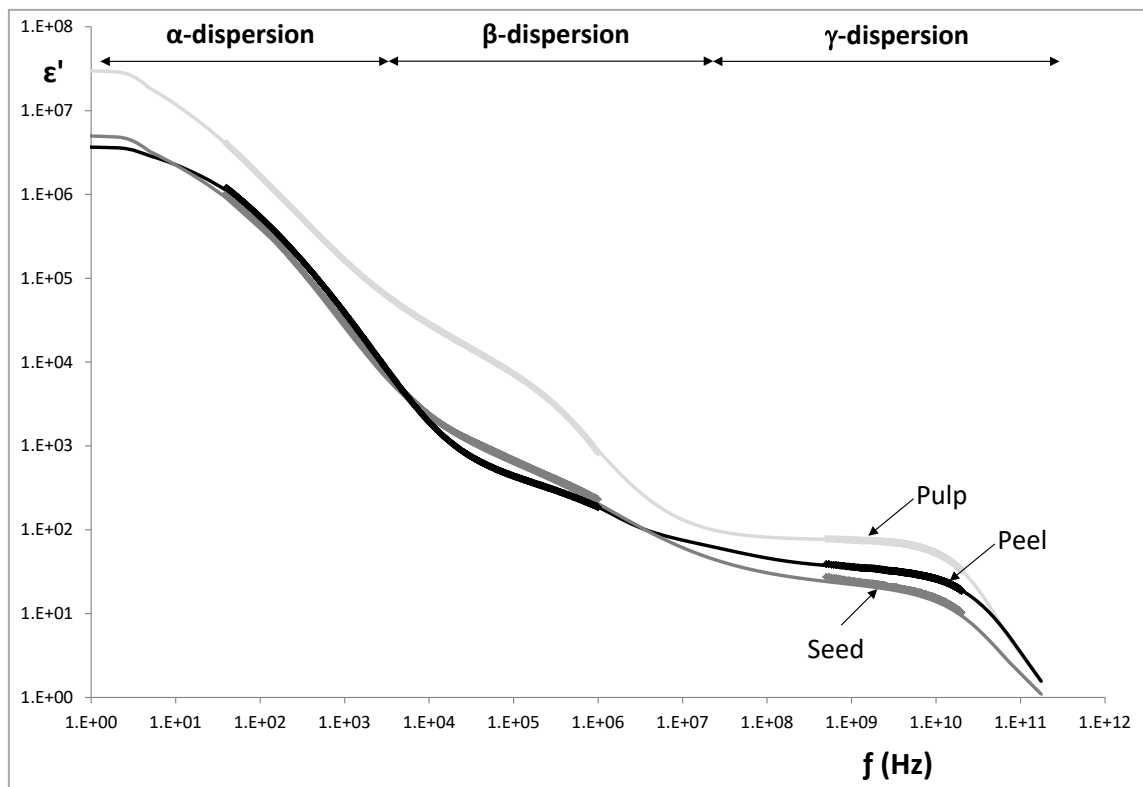


Fig. 3



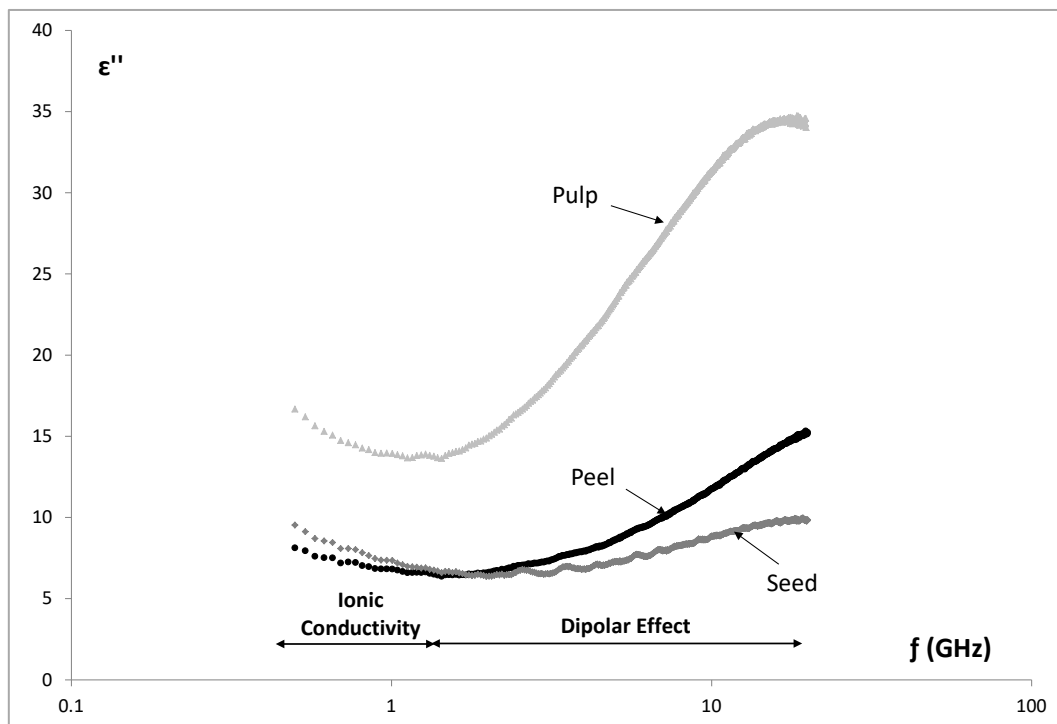


Fig. 4

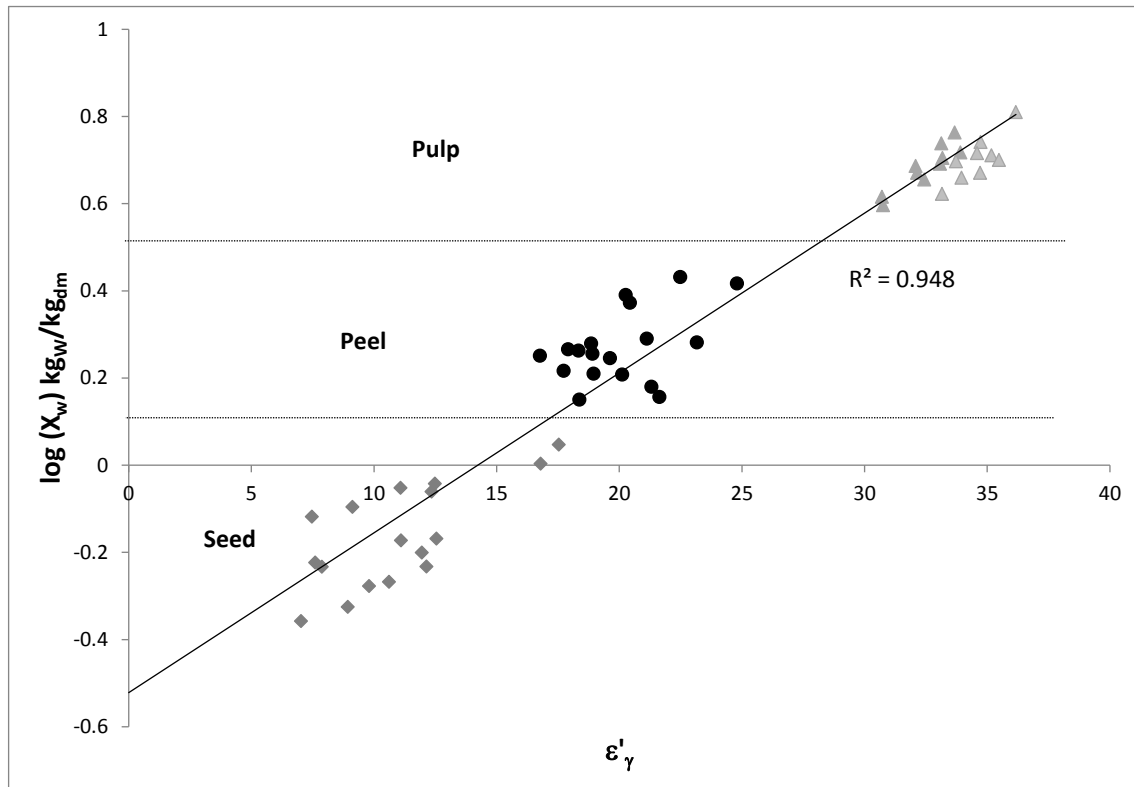


Fig. 5

**Table 1.** Physicochemical parameters of each mandarin tissue according to its maturity index (MI).

MI	Tissue	pH	X <sub>w</sub> (kg <sub>w</sub> /kg <sub>dm</sub> )	a <sub>w</sub>
10-15	Pulp	3.9 ± 0.3	5.490 ± 0.003 <sup>c</sup>	0.981 ± 0.003 <sup>c</sup>
	Peel		2.157 ± 0.008 <sup>b</sup>	0.976 ± 0.008 <sup>b</sup>
	Seed		0.722 ± 0.005 <sup>a</sup>	0.958 ± 0.005 <sup>a</sup>
15-20	Pulp	3.9 ± 0.2	4.8 ± 0.5 <sup>c</sup>	0.980 ± 0.005 <sup>c</sup>
	Peel		1.8 ± 0.4 <sup>b</sup>	0.9659 ± 0.0098 <sup>b</sup>
	Seed		0.7 ± 0.2 <sup>a</sup>	0.955 ± 0.005 <sup>a</sup>
20-25	Pulp	3.5 ± 1.4	5.1 ± 0.6 <sup>c</sup>	0.981 ± 0.003 <sup>c</sup>
	Peel		1.9 ± 0.4 <sup>b</sup>	0.967 ± 0.006 <sup>b</sup>
	Seed		0.67 ± 0.19 <sup>a</sup>	0.9526 ± 0.0096 <sup>a</sup>

Different letters (a-c) indicate significant difference among values of each tissue according to each MI

with  $p < 0.05$ .

**Table 2.** Relaxation dielectric constant at each specific dispersion ( $\alpha$ ,  $\beta$  and  $\gamma$ ).

MI	Tissue	$\epsilon'$								
		$\alpha (\cdot 10^4)$			$\beta (\cdot 10^2)$			$\gamma$		
10-15	Pulp	345	±	50 <sup>a</sup>	11	±	2 <sup>a</sup>	34.6	±	0.92 <sup>a</sup>
	Peel	5	±	0.4 <sup>b</sup>	1.8	±	0.15 <sup>b</sup>	16	±	4 <sup>b</sup>
	Seed	18	±	6 <sup>b</sup>	3	±	1 <sup>b</sup>	11	±	3 <sup>c</sup>
15-20	Pulp	304	±	56 <sup>a</sup>	13	±	4 <sup>a</sup>	34.2	±	0.8 <sup>a</sup>
	Peel	17	±	13 <sup>b</sup>	2.1	±	0.5 <sup>b</sup>	15	±	4 <sup>b</sup>
	Seed	20	±	8 <sup>b</sup>	2	±	1 <sup>b</sup>	10	±	3 <sup>c</sup>
20-25	Pulp	356	±	158 <sup>a</sup>	12	±	3 <sup>a</sup>	34	±	1 <sup>a</sup>
	Peel	6	±	2 <sup>b</sup>	1.6	±	0.3 <sup>b</sup>	15	±	2 <sup>b</sup>
	Seed	13	±	10 <sup>b</sup>	2	±	1 <sup>b</sup>	10	±	3 <sup>c</sup>

Different letters (a-c) indicate difference among values of each tissue according to each MI with  $p < 0.05$ .

**Table 3.** Relaxation frequency at each specific dispersion ( $\alpha$ ,  $\beta$  and  $\gamma$ ).

MI	Tissue	$f$					
		$\alpha$ (kHz)		$\beta$ (MHz)		$\gamma$ (GHz)	
10-15	Pulp	0.4	$\pm$ 0.3 <sup>c</sup>	0.9	$\pm$ 0.1 <sup>b</sup>	20	$\pm$ 3 <sup>a</sup>
	Peel	6.2	$\pm$ 0.7 <sup>a</sup>	2.2	$\pm$ 0.5 <sup>a</sup>	22	$\pm$ 4 <sup>a</sup>
	Seed	3	$\pm$ 1 <sup>b</sup>	1.2	$\pm$ 0.4 <sup>ab</sup>	18	$\pm$ 4 <sup>a</sup>
15-20	Pulp	0.4	$\pm$ 0.2 <sup>c</sup>	0.597	$\pm$ 0.093 <sup>b</sup>	18	$\pm$ 3 <sup>a</sup>
	Peel	5	$\pm$ 2 <sup>a</sup>	2	$\pm$ 0.7 <sup>a</sup>	24	$\pm$ 4 <sup>a</sup>
	Seed	4	$\pm$ 2 <sup>b</sup>	1.90	$\pm$ 0.5 <sup>ab</sup>	19	$\pm$ 2 <sup>a</sup>
20-25	Pulp	0.5	$\pm$ 0.3 <sup>c</sup>	0.63	$\pm$ 0.11 <sup>b</sup>	18	$\pm$ 2 <sup>a</sup>
	Peel	8	$\pm$ 1 <sup>a</sup>	2	$\pm$ 0.3 <sup>a</sup>	25	$\pm$ 5 <sup>a</sup>
	Seed	4.2	$\pm$ 0.9 <sup>b</sup>	2	$\pm$ 0.2 <sup>ab</sup>	19	$\pm$ 2 <sup>a</sup>

Different letters (a-c) indicate significant difference among values of each tissue according to each MI with  $p < 0.05$ .